Simulation of Viscoelastic and Plastic deformation of C-S-H of Cement Paste at very low (w/c) mass ratio

[1]Nasser Asroun and [*1]Aissa Asroun
[1]Civil Engineering and Environment Laboratory, Djillali Liabes University
PO box 89 Sidi Bel-Abbes 22000 Algeria

Abstract

In this work, a nanoindentation of cement paste trough a two-dimentional (2-D) axisymmetric model was investigated using the capacities of the ANSYS finite element (FE) code. The indentation process under consideration involves three forms of Calcium-Silicate-Hydrate (C-S-H) substrates indented by a rigid indenter under the condition of frictionless contact. For the 2-D model, the indenter has a half-angle of 70.3°, and thus has the same projected area-depth function as the standard Berkovich indenter. The model have the ability to simulate the trapezoidal load history, study the influence of mechanical properties of each form of C-S-H on indentation response and simulate the development of viscoelastic and plastic deformation during indentation. The simulation results agree well with the experimental ones and show that the Low Density (LD) form of C-S-H provides the maximum value of viscoelastic deformation and the higher plastic deformation normalized over the total deformation was observed in the Ultra High Density (UHD) form of C-S-H of cement paste.

Key words: Cement paste; nanoindentation; viscoelastic and plastic deformations.

1. Introduction

The nanoindentation is one of the most promising techniques that emerged from the implementation of nanotechnology in material science and engineering to assess mechanical properties at small scales. The idea is simple: by pushing a needle onto the surface of a material, the surface deforms in a way that reflects the mechanical properties of the indented material. Yet, in contrast to most metals and ceramics, for which this technique was originally developed, most materials relevant for civil engineering, petroleum engineering or geophysical applications, are highly heterogeneous from a scale of a few nanometers to macroscopic scales. The most prominent heterogeneity is the porosity.

Take, for instance, the case of concrete. Groundbreaking contributions date back to the 1950s with the work of Powers and his colleagues [1], who by correlating macroscopic strength [2] and stiffness data [3] with physical data of a large range of materials prepared at different w/c-ratios early on recognized the critical role of the C-S-H porosity (or gel porosity), respectively the C-S-H packing (“one minus porosity”) on the macroscopic mechanical behavior; in particular for cement pastes below a water-to-cement ratio of w/c<0.42, for which the entire porosity of the material is situated within the C-SH (no “capillary water” in Powers' terminology), and for which the hydration degree α of the hardened material is smaller than one. Powers considered the C-S-H gel porosity (gel pore volume over total gel volume) to be material invariant and equal to $\emptyset_0 = 0.28$ independent of mix proportions,

*Corresponding author: Address: Civil Engineering and Environment Laboratory, Djillali Liabes University PO box 89 Sidi Bel-Abbes 22000 ALGERIA. E-mail address: a_asroun@yahoo.fr, Phone: +213771358526 Fax: +21348554661

hydration degree, C-S-H morphology, etc. The application of advanced microscopy, X-ray mapping and Neutron scattering techniques to cement-based materials later on revealed that the assumption of a constant gel porosity could not be but an oversimplification of the highly heterogeneous nanostructure of cement-based materials, overlooking the particular organizational feature of cement hydration products in highly dense packed "inner" products and loosely packed "outer" products (see, for instance [4]). The quantitative translation of these morphological observations into a concise microstructure model of the gel microstructure is due to Jennings and co-worker [5], who recognized that outer and inner products are two structurally distinct but compositionally similar C-S-H phases; that is, amorphous nanoparticles of some 5 nm characteristic size pack into two characteristic forms, a Low Density (LD) C-S-H phase and a High Density (HD) C-S-H phase, that can be associated with outer and inner products.

The existence and mechanical importance of these phases have been confirmed by nanoindentation [6]: LD C-S-H and HD C-S-H were found to be uniquely characterized by a set of material properties that do not depend on mix proportions, type of cement, etc. Instead, they are intrinsic material invariant properties. The link between these mechanical C-S-H phase properties and C-S-H packing density has been established, showing that the C-S-H phases exhibit a unique nanogranular morphology [7], with packing densities that come remarkable close to limit packing densities of spheres; namely the random close-packed limit (RCP, [8]) or maximally random jammed state (MRJ, [9]) of $\eta \sim 0.64$ for the LD C-S-H phase; and the ordered face-centered cubic (fcc) or hexagonal close-packed (hcp) packing of $\eta = \pi/\sqrt{18} = 0.74$ [10] for the HD C-S-H phase. Recent study made by Ulm and all [11] was shown that the packing density distributions for different w/c provides strong evidence of three statistically significant C-S-H phases; namely a Ultra-High-Density (UHD) C-S-H phase, in addition to the already known LD C-S-H and HD C-S-H phases. The nanomechanical properties of the UHD C-S-H phase, M and H, are found to follow similar packing density scaling relations as LD C-S-H and HD C-S-H. This suggests that the UHD C-S-H phase is structurally distinct but compositionally similar to the other C-S-H phases. That is, it is made of the same elementary building block, the C-S-H solid, and differs from LD and HD C-S-H only in its characteristic packing density. The UHD C-S-H phase has a packing density of $\eta = 0.83 \pm 0.07$, which comes remarkably close to a two scale limit random packing of $0.64 + (1 - 0.64) \times 0.64 = 0.87$.

In order to gain a better understanding of the viscous and plastic deformations of the three phases of C-S-H of cement paste during the nanoindentation procedure, finite element modeling (FEM) was performed and discussed. The indentation modeling was performed with commercial ANSYS software.

2. Theory

2.1. Mathematical modeling

Using the Oliver and Pharr method [12], the elastic modulus of the indented sample can be inferred from the initial unloading contact stiffness, $S = dp/dh$, i.e., the slope of the initial portion of the unloading curve, as shown in Figure 1.

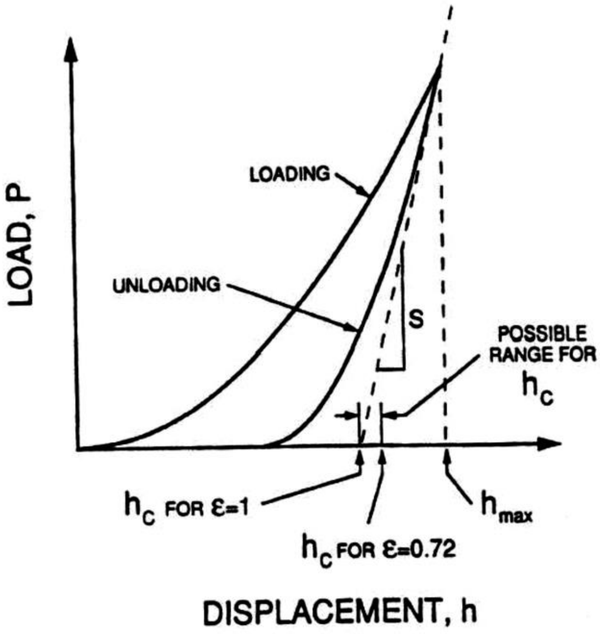

Figure 1. Loading and unloading curve

Based on the relationships developed by Snedden [13] for the indentation of an elastic half space by any punch that can be described as a solid of revolution of a smooth function, a geometry-independent relation involving contact stiffness, contact area, and elastic modulus can be derived as follows:

$$S = 2\beta\sqrt{\frac{A}{\pi}}E_r \tag{1}$$

Where β is a constant that depends on the geometry of the indenter. For Berkovich indenter, $\beta = 1.034$ and E_r is the reduced elastic modulus, which accounts for the fact that elastic deformation occurs in both the sample and the indenter. E_r is given by

$$\frac{1}{E_r} = \frac{1-\nu^2}{E} + \frac{1-\nu_i^2}{E_i} \tag{2}$$

Where E and ν are the elastic modulus and Poisson's ratio for the sample, respectively, E_i and ν_i are the same quantities for the indenter. For an indenter with a known geometry, the projected contact area is a function of the contact depth. The area function for a perfect Berkovich indenter is given by

$$A = f(h_c) = 24.56h_c^2 \tag{3}$$

Indenters used in practical nanoindentation testing are not ideally sharp. Therefore, tip geometry calibration or area function calibration is needed. A series of indentations is made on fused quartz at depths of interest. A plot of A versus h_c can be curve fit according to the following functional form

$$A = f(h_c) = 24.56h_c^2 + C_1h_c^1 + C_2h_c^{1/2} + C_3h_c^{1/4} + \cdots + C_8h_c^{1/128} \tag{4}$$

where C_1 to C_8 are constants. The lead term describes a perfect Berkovich indenter.

In case of analytical extraction of elastic properties through nanoindentation data it is possible to assess roughly the yield stress as being directly correlated with hardness value according to Tabor [14], and given by the following equation :

$$\sigma_y \approx {}^{H}\!/_{C} \tag{5}$$

where coefficient C can change in the range of 2.6-3.0.

2.2. Finite element modeling

The model consists of the simulation of nanoindentation test of cement paste on 2D planar model using the commercial finite element package ANSYS v.11.0 [15]. A Berkovich diamond indenter was used to perform the indentation test presented in this work. It had a pyramid shape with face angle of 65.27°. For simplicity purposes, the Berkovich indenter is commonly modeled as a conical indenter with a semi-apex angle of 70.3 degrees. This gives the same area to depth function as that of Berkovich indenter. A square area with dimensions including a base of 600 µm, a height of 600 µm was created to represent the cement paste specimens. The indenter and specimen are meshed by 2D structural PLANE182 element as shown in Figure 2.

Nodes along the centerline are constrained to move in *x*-direction and the nodes at the bottom line are constrained to move in *x* and *y*-directions. Axisymmetry conditions are applied along the centerline. The interaction of the indenter and the specimen is modeled as a contact pair with no friction. Contact element TARGET169 is applied to the Berkovich tip and CONTACT172 to the specimen. Load control technique is used to apply increasing load at maximum of 2 mN to the upper portion of the indenter in *y*-direction and the displacement in *y*-direction along the upper line of the specimen is measured.

For the diamond indenter an elastic linear isotropic model with Young modulus E_i =1141 GPa and Poisson ratio ν_i = 0.07 was used. For the cement paste, an elastic perfectly plastic material model with Von Mises yield criterion (σ_y) and Bilinear isotropic time hardening with implicit creep was chosen to extract the creep and plastic strains of the material.

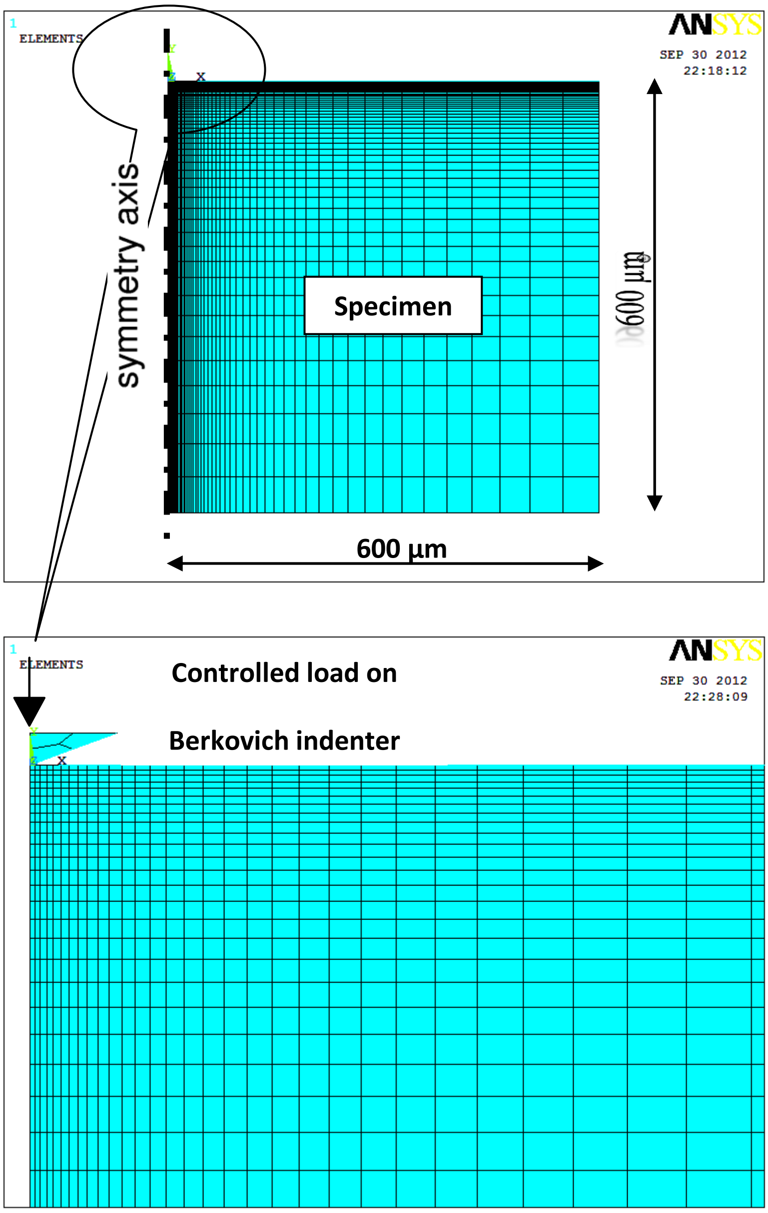

Figure 2. FE model of indenter and test specimens

Based on published cement properties, the Young's modulus, yield stress and Poisson's ratio of three forms of C-S-H phases (LD, HD and UHD) of cement paste prepared at very low w/c =0.15 mass ratio were presented in Table 1.

Table 1. Material properties of cement paste

Material	Young's modulus E(GPa)	Initial yield stress σ_y (GPa)	Poisson's Ratio ν
LD(C-S-H)[16]	25.3	0.198	0.24
HD(C-S-H)[16]	39.21	0.347	0.24
UHD(C-S-H)[16]	53.84	0.556	0.24

3. Results and discussion

The simulation results of indentation test of cement paste at nanoscale with the visco-elasto-plastic material model were presented in this section. The indentation depth is shown on X-axis and load on Y-axis. It can be observed that the maximum load of 2 mN obtained against maximum indentation depth of 405 nm, 320 nm and 255 nm for the LD, HD and UHD respectively of C-S-H phase were in good agreement with those of the experimental results of Vandamme and Ulm [17] shown in Figure 3.

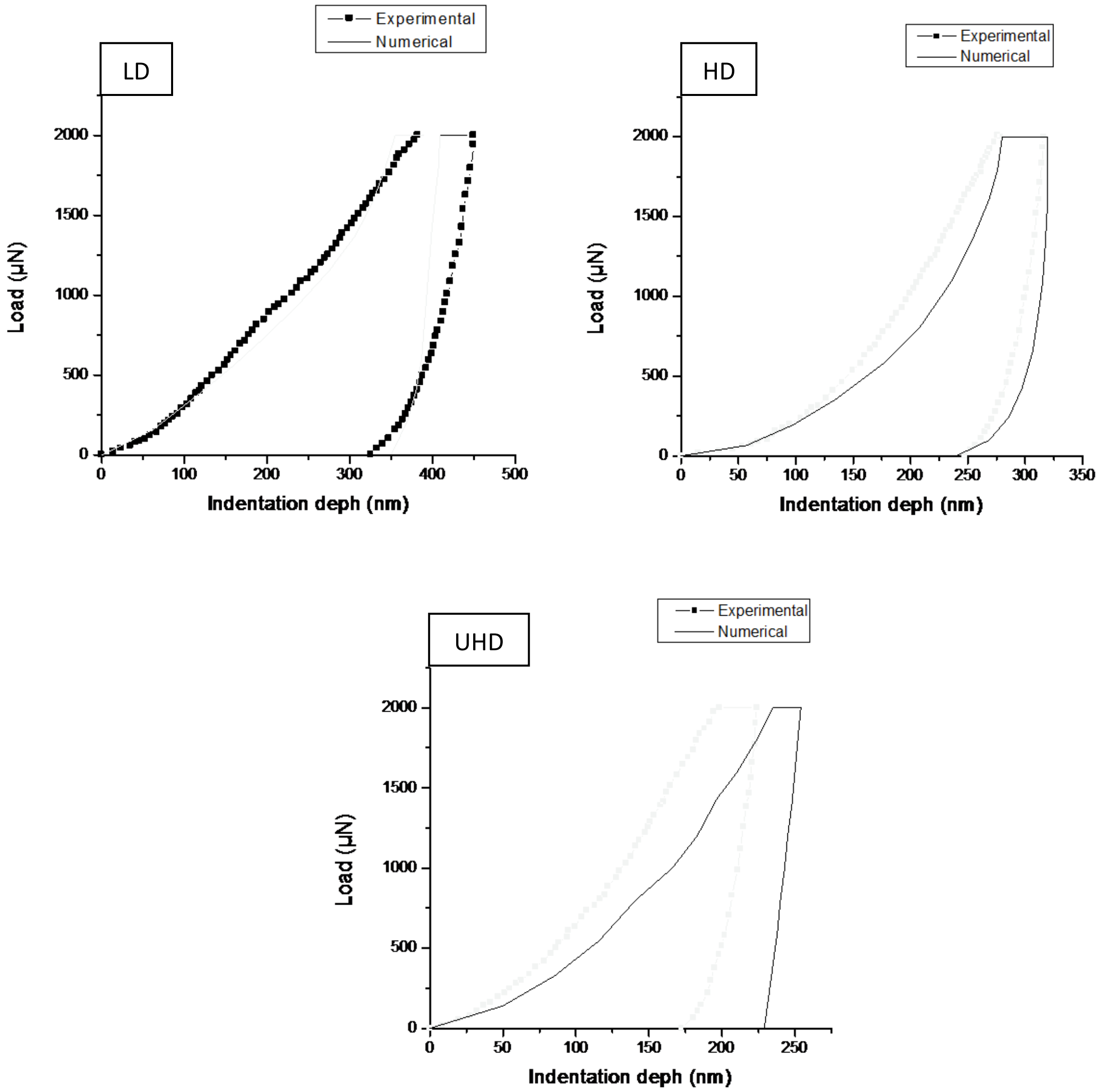

Figure 3. Load-indentation curves for LD, HD and UHD of C-S-H phase of cement paste

It reveals that model is able to capture the viscous strains for different forms of C-S-H showing that the higher value of viscous deformation was observed in the LD of C-S-H phase. This result remains logical since the LD of C-S-H posses the lower mechanical properties with indentation modulus of $M = 25.3\ GPa$ and indentation hardness of $H = 0.594\ GPa$. While the water available for hydration increases the amount of hydration solid, it appears that the concurrent increase in gel porosity favors the formation of looser packed LD C-S-H to the detriment of HD C-S-H; while the UHD C-S-H phase remains almost constant.

- A high w/c ratio entails an increase in the hydration degree. This increase is due an increase in similar proportions of both the C-S-H solid and the gel porosity; roughly 5% per Δ(w/c)=0.1 resulting in higher values of viscous deformation.
- A very low w/c=0.15 is characterized by a hydration degree on the order of α=0.6, a 10% gel porosity and a 50% C-S-H solid volume fraction, favors (almost) exclusively the formation of the UHD C-S-H phase [11].

A further study was conducted in order to studying the evolution of the plastic deformation for the different C-S-H forms of cement paste using the developed FE model. The plastic deformation normalized over the total deformation for each forms was extracted from the numerical and experimental curves as h_f/h_{max} . Figure 4 shows the comparison of the evolution of plastic deformation normalized over the total deformation for the three forms of C-S-H phase between the experiment and FEM. Normalized plastic deformation was found higher in the UHD forms of C-S-H phases of cement paste and was found lower in the HD forms of C-S-H phases. It was about 90% for the UHD forms and 75% for HD forms.

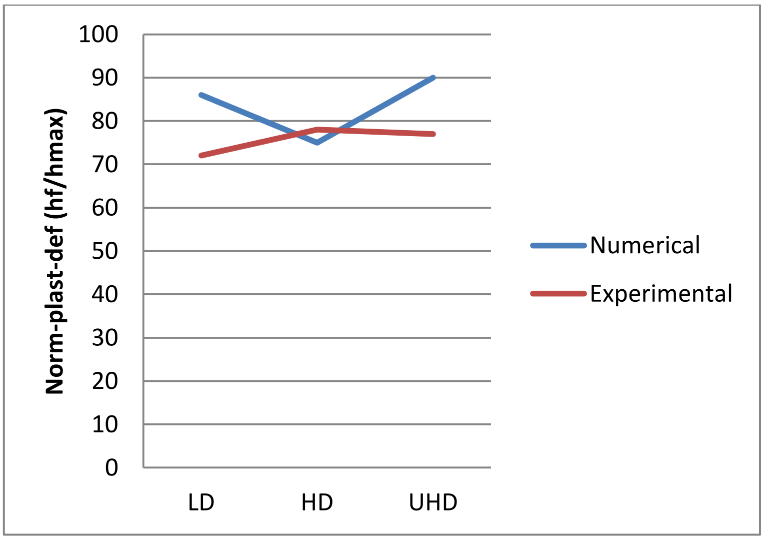

Figure 4. Normalized plastic deformation of different forms of C-S-H phases of cement paste

4. Conclusion

In this study, the response of nanoindentation test of cement paste was simulated by visco-elasto-plastic material model. The viscous and plastic deformations of the indentation test were investigated. The numerical and experimental results are compared, and the following conclusions are obtained :

1. The proposed model is able to reproduce the full indentation response of three forms of C-S-H phases of cement paste at nanoscale including viscous and plastic strains.

2. The viscous deformation was higher in the LD forms of C-S-H phases and was lower in the U-H-D forms of C-S-H phases of cement paste.
3. Normalized plastic deformation was higher in the U-H-D forms of C-S-H phases.
4. The load-indentation depth curves of numerical simulation agree well with the experimental ones while the elastic perfectly plastic properties are adopted in ANSYS.

5. Acknowledgement

This work was supported in part by the National Council of Evolution of University Projects of Research of Algeria under Grant number CNEPRU J0402120090080.

6. References

[1] T.C. Powers, T.L. Brownyard Studies of the physical properties of hardened Portland cement paste. Bull. 22, Res. Lab.of Portland Cement Association, Skokie, IL, U.S. J. Am. Concr. Inst. (Proc.). 43 (1947) 101-132, 249-336, 469-505,549-602, 669-712, 845-880, 933-992 (reprint).

[2] R.A. Helmuth, D.H. Turk, In Symp. Struct. Portland Cem. Paste Concr. 1966; 135.

[3] G. J. Verbeck, R.A. Helmuth, In 5th Int. Congress Cement Chemistry, Tokyo, Japan. 1969; 1.

[4] J.H. Taplin, Australian J. Appl. Sc. 1959; (10) 329.

[5] H. M. Jennings, Cem. Concr. Res., 2000; (30) 101.

[6] G. Constantinides, F.-J. Ulm, K. Van Vliet, Materials and Structures, 2003; 36(3) 191.

[7] G. Constantinides, F.-J. Ulm. Journal of the Mechanics and Physics of Solids, 2007; 55 (1) 64.

[8] H.M. Jaeger, S.R. Nagel, Science, 1992; 255(5051) 1523.

[9] A. Donev, I. Cisse, D. Sachs, E. A. Variano, F. H. Stillinger, R. Connely, S. Torquato, P. M. Chaikin, Science, 2004; 303 990.

[10] N. J. A. Sloane, Nature, 1998; 395 435.

[11] F. -J. Ulm, Convegno Nazionale IGF XX, Torino; 2009; 3-10

[12] Oliver W.C and Pharr G.M, 1992, An Improved Technique for Determining Hardness and Elastic Moduli using Load and Displacement Sensing Indentation Experiments, Journal of Materials Research, 7 (6), pp 1564-1583.

[13] Sneddon I.N., 1965, The Relation Between Load and Penetration in the Axisymmetric Boussinesq Problem for a Punch of Arbitrary Profile, International Journal of Engineering and Science, 3 (1), p. 47.

[14] Tabor D., 1948, A Simple Theory of Static and Dynamic Hardness. Proc. R. Soc. Lond. A, 192 (1), pp 247–274.

[15] ANSYS, 2011, Ansys Reference Manual version 11.0, Available via http://www.ansys.com.

[16] Vandamme M, 2008, The nanogranular origin of concrete creep: A nanoindentation investigation of microstructure and fundamental properties of calcium-silicate-hydrates, thesis of doctorate of philosophy.

[17] Vandamme M, Ulm F-J 2009), Nanogranular origin of concrete creep, PNAS paper, 106 (26), 10552–10557.